CHEMISTRY AND CLOUDS OF JUPITER'S ATMOSPHERE: A GALILEO PERSPECTIVE

S. K. ATREYA AND M. H. WONG
Department of Atmospheric, Oceanic, and Space Sciences
The University of Michigan, Ann Arbor, Michigan 48109-2143, USA

T. C. OWEN
Institute for Astronomy, University of Hawaii
Honolulu, Hawaii 96822, USA

AND

H. B. NIEMANN AND P. R. MAHAFFY
Goddard Space Flight Center, Greenbelt, Maryland 20771, USA

Abstract. The chemical processes responsible for the formation of minor trace species and the structure of clouds in Jupiter's atmosphere are discussed. Comparisons with relevant Galileo Probe and Orbiter measurements give important new insight into chemistry, thermodynamics, and meteorology in the atmosphere. A brief overview of the bulk atmospheric composition is included since it forms the basis for the chemical and cloud formation processes.

1. Composition

In 1932, Rupert Wildt identified methane and ammonia (CH_4 and NH_3) in the atmosphere of Jupiter. Identification of a few other molecules followed from ground-based spectroscopic observations. The two Voyager spacecraft determined the abundances of many molecules by remote sensing of Jupiter's atmosphere in 1979 and 1980. However, it was up to the Galileo Probe Mass Spectrometer (GPMS) to carry out the first in situ measurement of the composition of Jupiter's atmosphere to 20 bars in December 1995. Complementary remote sensing data on composition are being collected by the Galileo Orbiter Near Infrared Mapping Spectrometer (NIMS)

C. Barbieri et al. (eds.), The Three Galileos: The Man, The Spacecraft, The Telescope, 249–260.

and the Ultraviolet Spectrometer (UVS). As a result of the Galileo measurements, many new species have been identified for the first time, including sulfur (as hydrogen sulfide, H_2S) and the noble gases, whose isotopic ratios have been measured as well. The presently known composition of Jupiter's atmosphere is listed in Table 1.

The He/H_2 ratio is found to be 80% of that on the Sun (von Zahn and Hunten, 1996; Niemann *et al.*, 1996a). The atmospheric depletion of helium is believed to be the result of fractionation of helium from metallic hydrogen in the 1–3 megabar region, followed by the rain out of helium droplets toward the core of the planet. On the other hand, carbon and sulfur—whose principal reservoirs on Jupiter are in the form of CH_4 and H_2S—are found to be enhanced, respectively, by approximately a factor of 3 and 2.7 relative to their elemental ratios on the Sun (Niemann *et al.*, 1996a, 1997; Mahaffy, 1996). In the Galileo Probe region, the H_2O/H_2 mixing ratio is found to be ≤ 0.2 solar at 10 bar (Niemann *et al.*, 1996a) but it continues to increase with depth (Niemann *et al.*, 1996b). At least one interpretation of the Voyager infrared data implies $O/H = 1.5 \times$ solar (Carlson *et al.*, 1992). The Galileo Probe data on the deep atmospheric mixing ratios of NH_3 and PH_3 are still being analyzed, but the ground-based and pre-Voyager data for the shallower regions indicate N and P elemental ratios close to solar. The unexpected depletion of condensible volatiles (NH_3, H_2S, and H_2O) to great depths in the Probe entry region (Table 1) has important meteorological implications, as discussed later in the Clouds section. The enhancement of C/H and S/H relative to their values on the Sun appears consistent with the icy planetesimal hypothesis for the formation of Jupiter and the origin of its atmosphere. The elemental ratios and the noble gas isotopic ratios along with their implications for the origin of Jupiter's atmosphere are discussed in greater detail in the paper by Owen *et al.*, 1997 (this book).

Phosphine (PH_3), arsine (AsH_3), germane (GeH_4), and carbon monoxide (CO) are in thermochemical equilibrium at temperatures above 800–3000 K. Their detection in the stratosphere of Jupiter (Table 1)—where they are in disequilibrium—is indicative of a strong convection in Jupiter's interior which allows these species to be upwelled without chemical destruction along the way.

2. Photochemistry

On a globally averaged basis, chemistry triggered by the absorption of solar ultraviolet radiation is the dominant source of production of trace species in Jupiter's atmosphere. Other mechanisms—charged particles, lightning, cosmic rays—pale in comparison, but could be important locally. Amongst

TABLE 1. Composition of Jupiter's Atmosphere

Major Species	*Mixing Ratios*[1]	*Jupiter/Sun*[2]	*Remarks*[3]
H_2	0.865		
He	0.156±0.006	0.8	HAD; GPMS
Principal Minor Constituents			
H_2O	$\sim 2.6 \times 10^{-3}$	1.5	V/IRIS (5μm)
	$< 10^{-6}$ (<4 bar)		GPMS; NIMS
	$\leq 3.7 \times 10^{-4}$ (10 bar)	≤ 0.2	GPMS
	? (20 bar)	?	GPMS. Increasing in 10–20 bar
CH_4	$2.0 \pm 0.15 \times 10^{-3}$	3	GPMS; V/IRIS; Ground
	$2.5(+3/-2)\times10^{-5}$		V/UVS. At 1μb
C_2H_6	$1\text{–}5\times10^{-6}$		GPMS; V/IRIS; Ground
C_2H_2	$2\text{–}8\times10^{-8}$		V/IRIS; Ground. In stratosphere
	$< 2.5 \times 10^{-6}$		V/UVS. In 1–10μb
C_2H_4	$7 \pm 3 \times 10^{-9}$		GPMS; V/IRIS (N polar region)
C_3H_4	$2.5(+2/-1)\times10^{-9}$		V/IRIS (N polar region)
C_6H_6	$2(+2/-1)\times10^{-9}$		V/IRIS (N polar region)
NH_3	$2.3\text{-}2.9\times10^{-4}$	1-1.3	VLA mm-cm. Below NH3 clouds
	$\sim 0.2\text{-}1\times10^{-5}$		NFR; NIMS. 0.5–3 bar
H_2S	$(1\text{-}9)\times10^{-5}$	0.3-2.7	GPMS. In 8–20 bar
	$< 1 \times 10^{-6}$		GPMS. At < 4 bar
	$< 3.3 \times 10^{-8}$		Ground (2.7μm). At 0.8 bar
Disequilibrium Species			
PH_3	$(1\text{-}2)\times10^{-7}$		V/IRIS; CSO. In 0.2-0.6 bar
	6×10^{-7} (> 1 bar)	0.8	V/IRIS
CO	2×10^{-9}		Ground (5μm). In stratosphere
GeH_4	$7 \pm 2 \times 10^{-10}$		V/IRIS; Ground (5μm). NEB
AsH_3	$2.2 \pm 1.1 \times 10^{-10}$		IR; Ground. In stratosphere
Other Minor Constituents			
H	Variable		V/UVS; IUE; OAO
$(H_2)_2$	Variable		V/IRIS (28.2μm)
Noble Gases, and Isotopic Ratios			
He	0.156 ± 0.006	0.8	HAD; GPMS
^{20}Ne	$2.3 \pm 0.25 \times 10^{-5}$	0.1	GPMS
^{36}Ar	$1 \pm 0.4 \times 10^{-5}$	1–1.5	GPMS
^{84}Kr	$\leq 8.5 \pm 4 \times 10^{-9}$	≤ 5	GPMS
^{132}Xe	$\leq 5 \pm 2.5 \times 10^{-9}$	≤ 50	GPMS
$^{3}He/^{4}He$	$1.1 \pm 0.1 \times 10^{-4}$		GPMS
D/H	$2.2 \pm 0.5 \times 10^{-5}$		ISO (37μm). Footnotes 1 and 2
	$3.5 \pm 1.5 \times 10^{-5}$		GPMS. Footnotes 1 and 2
$^{12}C/^{13}C$	91		GPMS

[1 2 3]See footnote at the bottom of following page

the list of molecules detected on Jupiter, only NH_3 and CH_4 can result in any significant photochemical process since the other species are either condensed out or are inaccessible to the photolyzing flux, and H_2 is only dissociated into hydrogen atoms. We will discuss briefly the photochemistry of NH_3 and CH_4 below.

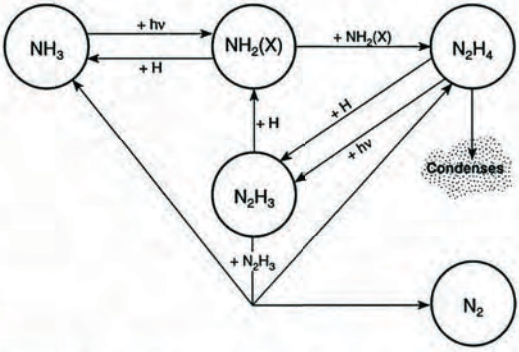

Figure 1. Schematic of ammonia photochemistry in Jupiter's atmosphere (after Atreya *et al.*, 1978).

The photolysis of NH_3 occurs at wavelengths below 230 nm in the upper troposphere and lower stratosphere (~30–300 mb), and eventually leads to the formation of nitrogen (N_2), as shown in Fig. 1. Atreya *et al.* (1977) and Atreya and Romani (1985) calculate the N_2 mixing ratio to be between 0.01 ppb and 1 ppb from this source, depending upon the degree of

[1]Mixing ratios are given relative to H_2 except for H_2 whose mole fraction is listed. C_2H_6 and C_2H_4 mixing ratios shown are for the stratosphere by V/IRIS and ground-based data; GPMS identifies these molecules to the deep atmospheric levels. ISO D/H is by Encrenaz *et al.* (1996), and GPMS by Mahaffy (1996). The GPMS value will be refined with the completion of ongoing laboratory studies of the GPMS Engineering Unit. VLA NH3 is by de Pater and Massey (1985). Consult Atreya (1986, Chapter 1) for all other references not cited here or in the text.

[2]Solar elemental ratios are taken from Anders and Grevesse (1989). For certain heavy elements, they are, relative to H: C= 3.62×10^{-4}; N= 1.12×10^{-4}; O= 8.51×10^{-4}; S= 1.7×10^{-5} (solar photosphere), 1.84×10^{-5} (meteorites); and P= 3.73×10^{-7}. D/H on the Sun now is zero. The jupiter D/H measurements are expected to establish the best protosolar value of D/H.

[3]HAD, GPMS, and NFR are, respectively, Helium Atmospheric Detector, Probe Mass Spectrometer, and Net Flux Radiometer on the Galileo Probe; NIMS is the Near Infrared Mapping Spectrometer on the Galileo Orbiter; V/IRIS and V/UVS are the Infrared and Ultraviolet/Spectrometers on Voyager; ISO is the Infrared Space Observatory of ESA; VLA is the Very Large Array in New Mexico; and IUE is the International Ultraviolet Explorer.

supersaturation of hydrazine (N_2H_4). On the other hand, if any N_2 were left over from the accretionary period, then between 0.6 and 10 ppm of N_2 from Jupiter's interior (depending upon the extent of iron catalysis in the conversion of N_2 to NH_3) may be introduced into Jupiter's atmosphere (Prinn and Olaguer, 1981).

Fig. 2 shows the chemical pathways following the photolysis of CH_4 at wavelengths below 160 nm (mainly at 121.6 nm because of the large solar flux at Lyman-alpha). Stable C_2 hydrocarbons, C_2H_6 (ethane), C_2H_2 (acetylene), and C_2H_4 (ethylene) are formed quickly in the 10 mb–1 μb region. Catalytic conversion of acetylene to polyacetylenes (diacetylene, C_4H_2, etc.) can occur. This chemistry is discussed in detail in Atreya (1986) and Bishop *et al.* (1997). Gladstone *et al.* (1996) have studied C_3 and C_4 chemistry in detail. The most abundant C_3 hydrocarbon is C_3H_8 (propane), which is formed principally by $H + C_2H_4 \rightarrow C_2H_5$, followed by $CH_3 + C_2H_5 \rightarrow C_3H_8$. According to this model, the propane mixing ratio ranges from as high as 1 ppm in the maximum production region (1 mb–1 μb) to $\sim$10 ppb at 10 bar. Methylacetylene and allene (C_3H_4) have mixing ratios comparable to propane in the stratosphere, but they drop to $\leq 10^{-14}$ at the 10 bar level. In the model, the most abundant C_4 hydrocarbon is found to be butane (C_4H_{10}; $C_2H_5 + C_2H_5 \rightarrow C_4H_{10}$), whose mixing ratio ranges from $\sim$0.1 ppm in the stratosphere to $\sim$1 ppb at 10 bar. There is also the likelihood of the formation of benzene (C_6H_6), as indicated by laboratory experiments and by the Voyager infrared observations (C_6H_6 = 2 ppb has been detected previously in the north polar region, Table 1).

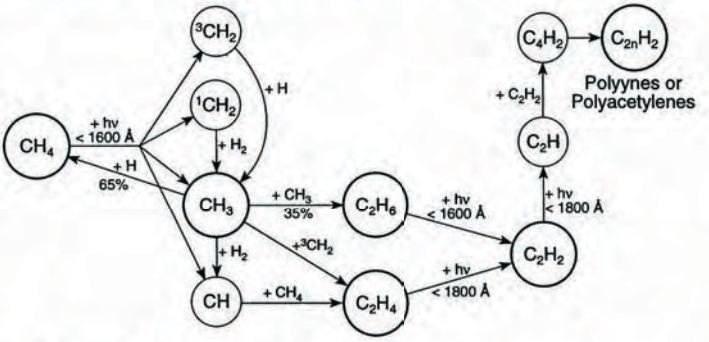

Figure 2. Schematic of methane photochemistry in Jupiter's atmosphere.

Coupling between the NH_3, CH_4, and PH_3 chemistries is at best weak in Jupiter's atmosphere (the PH_3 photolysis by itself is largely masked by

the much more abundant NH_3). The above coupling could form hydrogen cyanide (HCN), but many recent observations derive a low "upper limit" of 0.1 ppb for this species. On the other hand, several laboratory simulation experiments have predicted the formation of numerous heavy organic molecules (C-H and C-N-H groups), ranging to 10 or more carbon atoms (McDonald *et al.*, 1992, 1995).

It is clear from the above discussion that many more molecules than the two dozen listed in Table 1 may be present as a result of chemistry in Jupiter's atmosphere. A complete analysis of the Galileo Probe Mass Spectrometer data will allow an assessment of the complexity of this atmosphere. Although work on this is continuing, many new species have already been identified and measured. We show in Fig. 3 a typical mass spectrum taken at the 10 bar level. The molecules listed in Table 1 are identified. In addition, many other molecules suspected to be present are indicated by a "?" mark. There is scant evidence of diacetylene (C_4H_2 at 50 amu) or butane (C_4H_{10} at 58 amu), but propane (C_3H_8 at 44 amu) appears to be present at this pressure level. Note, however, that most of the signal at 44 amu can be attributed to CO_2 which is believed to be generated within the instrument during the pumping and gettering process (CS and N_2O, both at 44 amu are ruled out on the basis of isotopic and fragmentation pattern analysis). Another important point to note is that any heavy organic molecules that might be present are barely above the (very low) background level of 1–5 counts/integration period (Fig. 3). A special GPMS measurement integrated the signal from all molecules $\geq$150 amu, and found it also to be barely above the background. If heavy organic molecules are present, their mixing ratios must be less than a part per billion. We are presently studying the signal at 28 amu (C_2H_4, $?N_2$, ?CO), as well as other signatures in the mass spectra, as we continue laboratory recalibration using the flight spare mass spectrometer.

3. Clouds

The equilibrium cloud condensation model of Jupiter was first developed by Weidenschilling and Lewis (1973). Many changes and refinements to this model were made by Atreya and Romani (1985). According to this model, cloud layers of NH_3–ice NH_4SH–ice (ammonium hydrosulfide), H_2O–ice, and aqueous-ammonia solution are expected to form, respectively, at 0.7 bar (146 K), 2.2 bar (210 K), 5.4 bar (273 K), and 5.7 bar (277 K) for solar NH_3, H_2S, and H_2O, and at 0.8 bar (153 K), 2.4 bar (216 K), 5.4 bar (273 K), and 6.7 bar (290 K), respectively, if the abundance of NH_3, H_2S, and H_2O were 2 $\times$ solar. [Note that a gas phase chemical reaction between NH_3 and H_2S is believed to be responsible for the formation of NH_4SH,

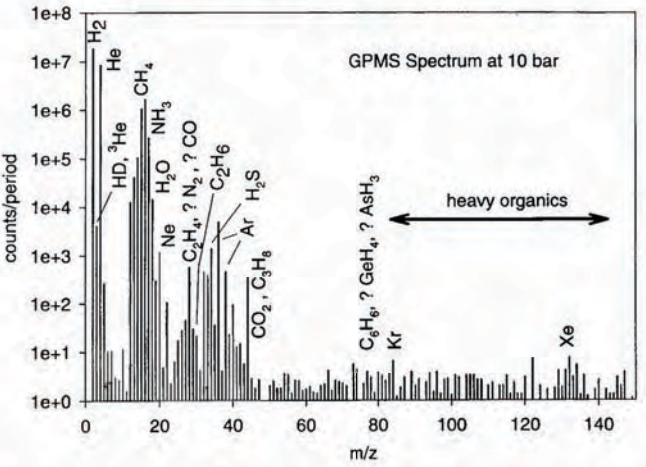

Figure 3. The GPMS spectrum is obtained by interpolating deadtime corrected detector counts for each mass to a Jupiter pressure of 10 bar. Molecules or noble gases which contribute to the spectrum are listed. Suspected contributions are indicated by a question mark.

which in turn solidifies at the above mentioned temperatures. There is also a suggestion that an ammonium sulfide, $(NH_4)_2S$, cloud could form instead (Owen and Mason, 1969; Ibragimov and Solodovnik, 1991). The laboratory chemical kinetics and thermodynamic data on the formation of these compounds is ancient and needs repeating.] The calculated cloud locations and concentrations are shown in Fig. 4a. In reality, cloud microphysical processes—including particle growth by coagulation and coalescence, followed by precipitation—are expected to reduce these model equilibrium cloud concentrations by factors of 3–10, if experience with the terrestrial cumulus cloud calculations is any indication of the process in Jupiter's atmosphere. However, the bases of the clouds (the lifting condensation levels) are expected to be well approximated by the model. Even after considering the microphysics, the Jovian cloud concentrations will be comparable to the cumulus clouds on Earth, according to this prediction.

With the exception of the topmost visible cloud of ammonia, remote sensing observations were not able to confirm or refute the existence of other cloud layers. The nephelometer on the Galileo Probe made the first in situ measurements of the clouds in Jupiter's atmosphere along the de-

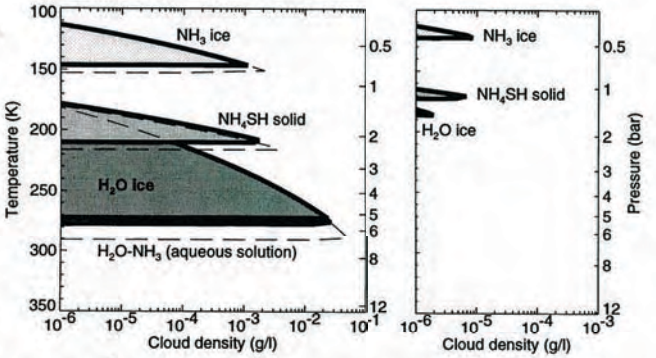

Figure 4. *(a, left)*: Equilibrium cloud model densities (in gram/litre) for solar and twice solar H_2O, H_2S and NH_3. The water cloud will form at 12 bars if O/H were 10 × solar. *(b, right)*: for $NH_3 = 2.24 \times 10^{-6}$ (0.01 solar), $H_2S = 1.85 \times 10^{-7}$ (0.005 solar), and $H_2O = 1.7 \times 10^{-7}$ (10^{-4} solar), which give results more similar to those measured in the Galileo Probe region. Temperature scale applies to Fig. 4a. See text for temperatures corresponding to the Probe region clouds shown in Fig. 4b.

scent trajectory of the Probe (Ragent *et al.*, 1996). Only one wispy cloud (optical depth, 1–2) was detected with certainty at ~1.34 bar (176 K). There is also a minimum in the data at 1.6 bar (185 K), and if it is due to a cloud, its opacity is far less than of the cloud at 1.34 bar. In addition, the Probe net flux radiometer (NFR) inferred indirectly a thin cirrus-type cloud layer (optical depth ~1) above the 0.5 bar level (136 K; Sromovsky *et al.*, 1996). Neither the locations nor the concentrations of the clouds detected by Galileo Probe have any resemblance whatsoever to the predictions shown in Fig. 4a. Furthermore, there is no evidence of a cloud where the putative water cloud is supposed to be. We believe that the seemingly divergent results of the model and the data could be reconciled, considering the unique nature of the Probe entry site.

Ground-based observations indicate that the Galileo Probe entered at the southern edge of, but well within, a 5-micron hot spot (Orton *et al.*, 1996). At this wavelength, Jupiter's spectrum is minimally affected by gaseous absorption, and the outgoing radiation is dominated by thermal emission rather than reflected sunlight. Therefore, the 5-μm radiation originates from deep in the troposphere, limited only by the opacity of H_2 and He gases—unit optical depth in H_2 occurs at the 6 bar level [the 5–μm hot spots typically cover 15% of the Probe entry latitude (6.5° N), Orton

et al., 1996]. The emission of radiation from deep in the atmosphere is an indicator of a relatively "clear," i.e. cloud-free atmosphere. This much was known about the nature of the hot spots, hence about the Probe entry site, pre-Galileo. The measurements of the condensible volatiles done on the Galileo Probe and the Orbiter provided the crucial evidence needed to understand the reason for the nearly cloud-free Probe trajectory.

The Probe net flux radiometer data are consistent with 1–2 × solar NH_3 between 3 and 6 bar level (Sromovsky *et al.*, 1996). The best fits to the data also require that the NH_3 mixing ratio drop by a factor of 20 between 3 and 1 bar, and by another factor of 4 between 1 and 0.5 bar. The Orbiter NIMS observations confirm the depletion of ammonia at lower pressures (Carlson *et al.*, 1996; Irwin *et al.*, 1996). The severe depletion of NH_3 to depths well below its expected condensation level of 0.7 bar seems surprising. Note the trend, however, that the mixing ratio continuously builds up with depth. A similar trend is seen in H_2S from measurements done with the Probe Mass Spectrometer. The "upper limit" on H_2S is 10^{-6} at $p \leq 4$ bar level, which is $< 1/30$ solar. At 8 bar, the H_2S mixing ratio is 0.3 solar, rising to solar at 10 bar and to 2.7 solar at ~20 bar (Mahaffy, 1996; Niemann *et al.*, 1997). Thus, like ammonia, H_2S is severely depleted to depths well below its expected condensation level of ~2 bar but builds up gradually with depth. The same trend is found for H_2O. At $p \leq 4$ bar, the H_2O mixing ratio ranges from 0 to an upper limit of 10^{-6}; the upper limit corresponds to $< 10^{-2}$ saturation (or $< 10^{-3}$ solar). This depletion in H_2O is also noted by the Galileo NIMS (Carlson *et al.*, 1996; Roos-Serot *et al.*, 1996). As in the case of H_2S and NH_3, H_2O shows signs of recovery with depth: ≤ 0.2 solar at 10 bar, and continuing to increase further with depth (Niemann *et al.*, 1996a, 1996b).

The highly depleted abundances of the condensible volatiles in the region of expected clouds are responsible for the lack of substantial clouds along the descent trajectory of the Galileo Probe into Jupiter's atmosphere. In Fig. 4b, we show an equilibrium cloud condensation simulation with cloud bases matching the observed cloud layers at 0.5 bar, 1.34 bar, and 1.6 bar levels. These clouds are identified with NH_3 – ice, at 0.5 bar, assuming an NH_3 mixing ratio of 2.2×10^{-6} (0.01 solar), with an NH_4SH–ice cloud at 1.34 bar, assuming an H_2S mixing ratio of 1.8×10^{-7} (5×10^{-3} solar), and with an H_2O – ice cloud at 1.6 bar, assuming an H_2O mixing ratio of 10^{-4} solar. These mixing ratios are consistent with those implied by the Galileo Probe and Orbiter data discussed above. (Note that the required H_2S mixing ratio lies between the GPMS upper limit of 10^{-6} at 4 bar and the upper limit of 3.3×10^{-8} down to the 0.8 bar level derived from ground-based 2.7-μm observations, Larson *et al.*, 1984). The calculated cloud concentrations in Fig. 4b are greater than observed by a factor

of 3–5. Even this level of agreement is good, considering that the equilibrium cloud condensation model predicts the lifting condensation level for a rising column of air, and the dynamics and microphysical processes are decidedly more complex than this simple scenario.

A plausible explanation for the greatly depleted abundances of the condensible volatiles to depths well below their expected condensation levels is that local meteorology in the Probe entry region controls their behavior (Atreya *et al.*, 1996; Owen *et al.*, 1996). We illustrate this scenario in Fig. 5. According to this scenario, the "normal" Jovian air—in which NH_3, H_2S, and H_2O are in their expected solar/supersolar mixing ratios—rises in a cell of "updraft." As it rises, the condensible volatiles begin to get depleted, first by condensation and precipitation, and then they are saturation limited as the air rises to cooler temperatures. This cold, dried-out air from which the condensible volatiles have been largely wrung out then descends in an adjacent cell of "downdraft," mixing with the local air there. It is in such a downdraft region that we believe the Galileo Probe descended. As the downdraft mixes with the air in the Probe region, the mixing ratios of the condensible volatiles begin to build up and reach their normal solar/supersolar values at some deep atmospheric pressure levels. Indeed, the Probe data discussed above show exactly this type of behavior for at least NH_3 and H_2S. Even for H_2O, the trend of gradual recovery with depth has been recorded; the exact mixing ratio reached at the deepest level is not yet fully constrained, however. The above updraft–downdraft scenario is somewhat similar to the Hadley circulation cell between the equator and subtropics on the Earth; the latter however describes a much larger scale phenomenon. One important point to note in the context of Jupiter's condensible volatiles is that they do not all level off at the same pressure level in the atmosphere (NH_3 between 3 and 6 bar, H_2S at $\sim$20 bar; H_2O ?). Neither do they recover to their expected solar/supersolar values immediately below their respective condensation levels, as would be expected if Jupiter's large internal heat source resulted in rapid mixing of these volatiles. There are at least a couple of different ways the downdraft could still persist to deep levels and allow the recovery of the condensible volatiles at different depths. First, the planetary distribution of Jupiter's internal heat may be nonuniform—in fact, Voyager data show that more of it is emitted at high latitudes than at the equator. Alternatively, Showman and Ingersoll (1996) have proposed a thermodynamic heat engine in reverse, which allows the downdraft to remain dry far below the condensation levels and for it to persist to great depths. As for the observed levelling off of the condensible volatile mixing ratios at different depths, we suggest that there is a likelihood of horizontal or lateral mixing of volatiles into the Probe region, in addition to the vertical mixing discussed above. It is also possible that

there is a multitude of updraft–downdraft cell pairs within the larger 5-μm hot spot of the Probe region, all interacting and eventually controlling the abundances of condensible volatiles in the Probe region. The dynamics of this region is expected to be complex, but it appears to us that the basic idea of local meteorology involving downdraft will hold since it explains both the behavior of the condensible volatiles with depth and the resulting cloud characteristics in the Probe entry region.

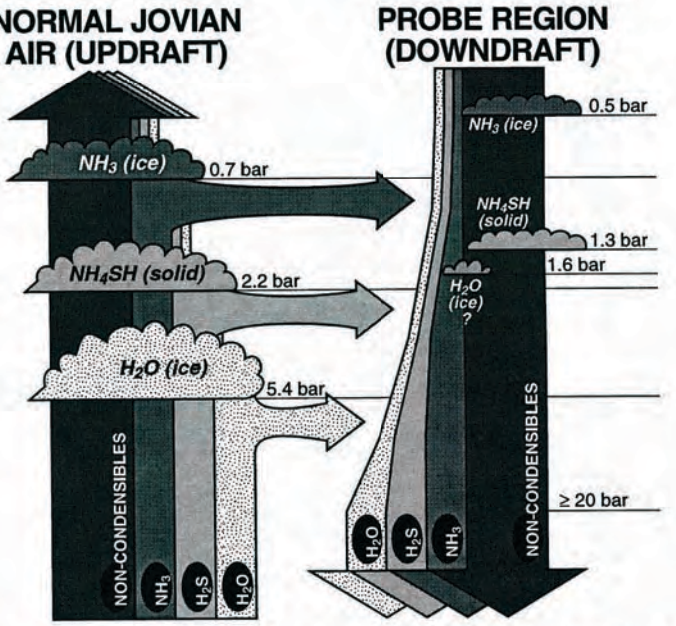

Figure 5. The effect of local meteorology on the condensible volatile abundances encountered by the Galileo Probe. The widths of vertical arrows are indicative of mixing ratios of gases at the given pressure level. Normal solar/supersolar Jovian air rises in the column on the left (updraft). Cloud base levels are given for solar elemental ratios. After condensation and precipitation, the rising air column is depleted of the condensible volatiles. For example, the saturation mixing ratios at 0.5 bar would be approximately $NH_3 = 10^{-7}$, $H_2S = 10^{-11}$, and $H_2O = 10^{-12}$. This desiccated air then descends into the Probe region (downdraft). On mixing with the Probe region air, the condensible volatile mixing ratios gradually recover to their deep atmospheric values. As expected, the resulting clouds in the Probe region (shown on the right) will be tenuous. The composition of the sinking air may be modified by lateral mixing, as implied by horizontal arrows. Three arrows for the three condensible volatiles indicate the atmospheric levels below which lateral mixing would be capable of significantly enriching the air in the downdraft.

The Galileo observations have demonstrated that we have come a long way since Galileo Galilei muttered at his inquisition his famous words, *"e pur, si muove"*—"even so, it does move." What we are seeing today is the result of the continuation of innovations begun by this great scientist nearly four centuries ago. The authors of this paper acknowledge support received from the Galileo Project. S. K. Atreya acknowledges support also from NASA's Planetary Atmospheres Program and T. C. Owen from NASA's Exobiology and Astronomy Programs for further analysis and interpretation of the observations.

References

Atreya, S. K. (1986) *Atmospheres and Ionospheres of the Outer Planets and their Satellites*. Springer-Verlag, New York and Berlin.
Atreya, S. K., Romani, P. N. (1985) in *Planetary Meteorology* (G. E. Hunt, ed.) Cambridge Univ. Press, pp. 17-68.
Atreya, S. K., Donahue, T. M., Kuhn, W. R. (1977) *Icarus*, **31**, 348–355.
Atreya, S. K., Donahue, T. M., Kuhn, W. R. (1978) *Science*, **201**, 611–613.
Atreya, S. K., Owen, T. C., Wong, M., Niemann, H. B., Mahaffy, P. (1996) *Bull. Am. Astron. Soc.*, **28**, No. 3, 1133.
Bishop, J., Romani, P. N., Atreya, S. K. (1997) *Planet Space Sci.*, in press.
Carlson, B. E., Lacis, A. A., Rossow, W. B. (1992) *Astrophys. J.* **388**, 648.
Carlson, R., *et al.* (1996) *Science*, **274**, 385–388.
dePater, I., Massie, S. T. (1985) *Icarus*, **62**, 143–171.
Encrenaz, T. *et al.* (1996) *Astron. Astrophys.* , **315**, L397–L400.
Gladstone, G. R., Allen, M., Yung Y. L. (1996) *Icarus*, **119**, 1–52.
Ibragimov, K. Y., Solodovnik, A. A. (1991) *Kinematika i Fizika Nebesnykh Tel*, **7**, 58.
Irwin, P. G., *et al.* (1996) *Bull. Am. Astron. Soc.*, **28**, 1135.
Larson, H. P., Davis, D. S., Hoffman, R., Bjoraker, G. (1984) *Icarus*, **60**, 621–639.
Mahaffy, P. R., (1996) *EOS*, Trans. Suppl., **77** (46), F438.
McDonald, G. D., Khare, B. N., Sagan, C. (1995) *Bull. Am. Aston. Soc.*, **27**, 1141.
McDonald. G. D., Thompson, W. R., Sagan, C. (1992) *Icarus*, **99**, 131–142.
Niemann, H. B., Atreya, S. K., Carignan, G., Donahue, T. M., Hartle, R., Haberman, J., Harpold, D., Hunten D., Kasprzak, W., Mahaffy, P., Owen, T., Spencer, N., Way, S. (1996a) *Science*, **272**, 846–848.
Niemann, H. B., *et al.* (1996b) COSPAR Meeting, Birmingham, England.
Niemann, H. B., *et al.* (1997) In preparation.
Orton, G., *et al.* (1996) *Science*, **272**, 839–840.
Owen, T. C. and Mason, H. P. (1969) *J. Atmos. Sci.* **26**, 870–873.
Owen, T. C., Atreya, S. K., Niemann, H. B., Mahaffy, P. (1996) *EOS*, Trans. Suppl., **77**(46), F438.
Owen, T. C., Atreya, S. K., Mahaffy, P., Niemann, H. B., Wong, M. H. (1997) This book.
Prinn, R. G. and Olaguer, E. P. (1981) *J. Geophys. Res.* **86**, 9895–9899.
Ragent, B., Colburn, D. S., Avrin, P., Rages, K. A. (1996) *Science*, **272**, 854–855.
Roos-Serot, M., Drossart, P., Encrenaz, T., Carlson, R., Baines, K., Orton, G. (1996) *Bull. Am. Astron. Soc.* **28**, No. 3, 1135.
Showman, A. P., Ingersoll, A. P. (1996) *Bull. Am. Astron. Soc.*, **28**, No. 3, 1141.
Sromovsky, L. A., Best, F. A., Collard, A. D., Fry, P. M., Revercomb, H. E., Freedman, R. S., Orton, G. S., Hayden, J. L., Tomasko, M. G., Lemmon, M. T. (1996), *Science*, **272**, 851–853.
von Zahn, U., Hunten, D. M. (1996) *Science*, **272**, 849–850.
Weidenschilling, S. J., Lewis, J. S. (1973) *Icarus*, **20**, 465–476.